protein family or genome annotation effort. Importantly, phylogenetic reconstruction is critical to synthesizing, from the growing wealth of sequence data, a more comprehensive view of genome evolution.

Methods

Data collation and analysis

Our analysis involved a set of 28 loci that had been proposed as instances of bacteria–vertebrate HGT, and for which PCR had been used to verify their presence in the human genome[5]. Each protein sequence was searched using the appropriate BLASTP or TBLASTN[14] algorithm against the following databases downloaded on 19 February 2001 from NCBI: non-redundant proteins; EST others nucleotides (GenBank non-mouse and non-human EST entries); unfinished microbial genome nucleotides; and the complete genome sequences of the nematode *C. elegans* and the insect *Drosophila melanogaster*. ClustalW[15] was used to align the resulting set of significant homologues, and the alignments were then refined by eye using the GCG or GeneDoc sequence editors. In several instances BLAST searches resulted in a large number of homologous sequences, which served as input for a preliminary phylogeny designed to assess paralogy (sequence homology due to gene duplication) and orthology (sequence homology due to speciation). This tree then served as a framework on which to exclude the more distantly related paralogues in a follow-up alignment and phylogeny. All potentially ambiguous gaps (that is, those involving complex insertion or deletion events) were removed before phylogenetic analysis. We coded all remaining gaps as missing data.

The amino-acid sequence alignments were analysed using maximum parsimony and neighbour joining, as implemented in the phylogenetic package PHYLIP[16]. Parsimony analyses randomized the input order 20–50 times, depending on the number of sequences in the alignment (that is, greater number of random additions for larger alignments). The distance matrixes that served as input for neighbour-joining analyses were calculated using the point-accepted-mutation (PAM) Dayhoff substitution model. Clade strength was assessed with bootstrap, using 1,000 replications. The alignments are available in Supplementary Information.

Phylogenetic principles for accepting or rejecting HGT

The branching arrangement of the resulting phylogenies is a critical component of an HGT assessment. In the case of a gene transfer from bacteria to vertebrates, the necessary phylogeny would show eukaryote paraphyly with vertebrates separated from non-vertebrates by a paraphyletic (a group that contains some but not all of the descendents of a common ancestor) assemblage of bacterial lineages, where some of the bacteria were more closely related to vertebrates than other bacteria, and in which most (or all) of available bacterial sequences form a clade with vertebrates (Fig. 1a). Horizontal gene transfer of the opposite direction (vertebrate–bacteria) would be expected to have a topology in which one or a few bacteria were sister group to the vertebrates, joined next by non-vertebrate taxa, and the remaining bacteria (if any) were outside this clade (Fig. 1b). Both such trees would need a root, which could come from Archaea or a paralogous gene. The clearest phylogenetic rejection of proposed bacteria–vertebrate HGT would involve eukaryotic monophyly, with a non-vertebrate eukaryote contained within that clade (Fig. 1c, d). Another example of phylogenetic rejection would include the respective monophylies of Archaea, Eucarya and Bacteria (or conversely, just Eucarya and Bacteria) in a tree rooted at a paralogous sequence, but with only vertebrates represented as eukaryotes (that is, bacterial monophyly negates the bacteria–vertebrate HGT hypothesis; Fig. 1e). Several ambiguous cases could arise, the most likely relating to the absence of non-vertebrate orthologous genes. A paraphyletic group of bacteria forming a clade with vertebrates, joined next by either Archaea or a paralogous gene family, could be a consequence of the poor representation of non-vertebrate genomes in contemporary databases, or could reflect an actual HGT from bacteria to vertebrates (Fig. 1f). The absence of a sequence from either a nematode (*C. elegans*) or fruit fly (*D. melanogaster*)—whose nearly complete genomes are available—in such a topology is not sufficient evidence to conclude bacteria–vertebrate HGT. Until a much broader sampling of non-vertebrate genomes are completed these cases should remain ambiguous.

1. Gray, M. W. The endosymbiont hypothesis revisited. *Int. Rev. Cytol.* **141**, 233–357 (1992).
2. Nelson, K. E. *et al.* Evidence for lateral gene transfer between Archaea and Bacteria from genome sequence of *Thermotoga maritima*. *Nature* **399**, 323–329 (1999).
3. Ruepp, A. *et al.* The genome sequence of the thermoacidophilic scavenger *Thermoplasma acidophilum*. *Nature* **407**, 508–513 (2000).
4. Doolittle, W. F. Phylogenetic classification and the universal tree. *Science* **284**, 2124–2128 (1999).
5. International Human Genome Sequencing Consortium. Initial sequencing and analysis of the human genome. *Nature* **409**, 860–921 (2001).
6. Smith, M. W., Feng, D.-F. & Doolittle, R. F. Evolution by acquisition: the case for horizontal gene transfers. *Trends Biochem.* **17**, 489–493 (1992).
7. Logsdon, J. M. Jr & Faguy, D. M. Evolutionary genomics: *Thermotoga* heats up lateral gene transfer. *Curr. Biol.* **9**, R747–R751 (1999).
8. Brunner, H. G., Nelen, M., Breakefield, X. O., Ropers, H. H. & van Oost, B. B. A. Abnormal behavior associated with a point mutation in the structural gene for monoamine oxidase A. *Science* **262**, 578–580 (1993).
9. Cases, O. *et al.* Aggressive behavior and altered amounts of brain serotonin and norepinephrine in mice lacking MAOA. *Science* **268**, 1763–1766 (1995).
10. Deckert, J. *et al.* Excess of high activity monoamine oxidase A gene promoter alleles in female patients with panic disorder. *Hum. Mol. Genet.* **8**, 621–624 (1999).
11. Brown, J. R. & Doolittle, W. F. Archaea and the prokaryote–eukaryote transition. *Microbiol. Mol. Biol. Rev.* **61**, 456–502 (1997).
12. Kyrpides, N. C. & Olsen, G. J. Archaeal and bacterial hyperthermophiles—horizontal gene exchange or common ancestry? *Trends Genet.* **15**, 298–299 (1999).
13. Eisen, J. A. Phylogenomics—improving functional predictions for uncharacterized genes by evolutionary analysis. *PCR Methods Appl.* **8**, 163–167 (1998).
14. Altschul, S. F. *et al.* Gapped BLAST and PSI-BLAST: a new generation of protein database search programs. *Nucleic Acids Res.* **25**, 3389–3402 (1997).
15. Thompson, J. D., Higgins, D. G. & Gibson, T. J. CLUSTAL W: improving the sensitivity of progressive multiple sequence alignment through sequence weighting, positions-specific gap penalties and weight matrix choice. *Nucleic Acids Res.* **22**, 4673–4680 (1994).
16. Felsenstein, J. PHYLIP (Phylogeny Inference Package) version 3.6. (Department of Genetics, University of Washington, Seattle, 2000).

··

Divergent sexual selection enhances reproductive isolation in sticklebacks

Janette Wenrick Boughman

Department of Zoology, University of British Columbia, Vancouver BC V6T 1Z4, Canada

··

Sexual selection may facilitate speciation because it can cause rapid evolutionary diversification of male mating signals and female preferences. Divergence in these traits can then contribute to reproductive isolation[1–3]. The sensory drive hypothesis predicts that three mechanisms underlie divergence in sexually selected traits[4]: (1) habitat-specific transmission of male signals[5–7]; (2) adaptation of female perceptual sensitivity to local ecological conditions[8]; and (3) matching of male signals to female perceptual sensitivity[4,9]. I test these mechanisms in threespine sticklebacks (*Gasterosteus* spp.) that live in different light environments. Here I show that female perceptual sensitivity to red light varies with the extent of redshift in the light environment, and contributes to divergent preferences. Male nuptial colour varies with environment and is tuned to female perceptual sensitivity. The extent of divergence among populations in both male signal colour and female preference for red is correlated with the extent of reproductive isolation in these recently diverged species. These results demonstrate that divergent sexual selection generated by sensory drive contributes to speciation.

Sexual selection can act through sensory drive to favour different mating signals and preferences in different environments. The sensory drive hypothesis predicts three mechanisms that may cause such divergence. First, females are likely to prefer conspicuous signals. Because habitat influences the physics of signal transmission, relative conspicuousness of signals should vary with habitat[4]. With visual signals, conspicuousness is enhanced when a signal differs from the background light. In relatively clear, fresh water, blue and red are high-contrast signal colours[10]. In tea-stained fresh water, red signals are likely to be masked by the redshifted background light, but black should be high contrast[11]. Second, perceptual sensitivity should vary with habitat[8,12] and lead to variation in preference. For example, the spectral quality of ambient light is likely to influence colour perception[12]. Several sources of selection may favour perceptual systems that work effectively in the local environment, because the visual environment can affect prey and predator detection as well as mate detection[12,13]. Third, male signals that match female perception are easier to detect and

should be preferred by females[4,9]. Over evolutionary time, the effect of habitat on signal conspicuousness and female perception can lead to divergent signals, perceptual sensitivity, and even female preference. Initial divergence would occur most readily in allopatric populations but could continue in sympatry. This divergence can contribute to reproductive isolation and ultimately to speciation.

Given that habitats differ in water colour, which affects the transmission of colour signals, I tested the following predictions of sensory drive: that male nuptial colour varies in correlation with this variation in habitat; that female perception also varies with habitat; and that signal variation matches perceptual variation. I then tested two predictions of the 'speciation by sexual selection' hypothesis: that mate preferences diverge, and that divergence in mating signals and preferences contribute to reproductive isolation. I studied six populations of recently diverged threespine sticklebacks from four lakes in coastal British Columbia, Canada: Paxton and Cranby lakes on Texada Island, and Enos and Brannen lakes on Vancouver Island. Two lakes (Paxton and Enos) each contain two reproductively isolated ecotypes of sticklebacks, benthics and limnetics. Benthics feed on macro-invertebrates and mate in the vegetated areas of the littoral zone, whereas limnetics feed on plankton in the open water and mate in the unvegetated areas of the littoral zone at shallower depths than the benthics[14,15]. The other two lakes (Cranby and Brannen) have a single type of stickleback whose pattern of habitat use is intermediate between the limnetic and benthic ecotypes. All lake sticklebacks have descended from marine ancestors since the Pleistocene epoch. Benthics and limnetics are probably the result of separate freshwater invasions[16] and may have been slightly diverged before first contact. Divergence among populations is so recent that little genetic incompatibility has built up, and postmating isolation is primarily ecological[17].

The nesting habitats of the six populations differ in water colour[14,15] (Fig. 1), which is probably caused by differences in the amount of decaying organic matter and the extent of vegetative cover. The two limnetics (Paxton and Enos) live in the least redshifted habitat, which is similar to the Paxton benthic habitat (λp50 (the median wavelength in a spectral scan) Paxton limnetic = 596 nm; Enos limnetic = 607 nm; Paxton benthic = 611 nm; pooled standard error = 4.9). The two solitary types (Cranby and Brannen) and Enos benthics live in significantly more redshifted habitats (λp50 Enos benthic = 620 nm; Cranby = 619 nm; Brannen = 627 nm; pooled standard error = 5.4; least significant difference = 10.3).

I scored two aspects of male nuptial colour: area and intensity of red coloration. Populations differ in red area (Fig. 1a; $F_{5,162}$ = 166.3, $P < 0.0001$) and red intensity (Paxton limnetic = 2.5; Enos limnetic = 2.7; Paxton benthic = 2.3; Enos benthic = 0.11; Cranby = 0.92; Brannen = 0.14; $F_{5,160}$ = 87.1, $P < 0.0001$). Area and intensity of red coloration correlate with the extent of redshift in background light (rank correlation coefficient: area, $r = -1.0$, $n = 6$, $P < 0.01$ (Fig. 1); intensity, $r = -0.94$, $n = 6$, $P < 0.05$). Thus, males display nuptial colours that are likely to contrast with the water colour of the habitat in which they mate and thus transmit readily, confirming the first prediction of sensory drive.

Using the optomotor response[18] I found differences between populations in female detection thresholds for red light ($F_{5,443}$ = 32.1, $P < 0.0001$). A lower threshold implies higher sensitivity. Limnetic females in both Paxton and Enos lakes are more sensitive to red than benthic females ($F_{1,438}$ = 16.2, $P < 0.0001$). Females from populations with red males are more sensitive to red light than females from populations with black males ($F_{1,438}$ = 18.0, $P < 0.0001$). This perceptual variation correlates with variation in water colour (Fig. 1b; $r = 0.94$, $n = 6$, $P < 0.05$), suggesting that the environment strongly influences perceptual sensitivity, confirming
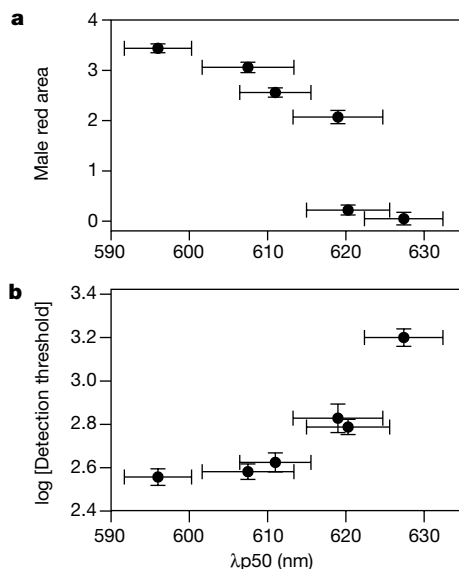

Figure 1 Influence of water colour (λp50 values for nesting habitat) on sexually selected traits in males and females. Values given are population means ± standard error (also for Figs 2 and 3). λp50 provides an index of dominant water colour. **a**, Area of red coloration in males correlates negatively to λp50 ($r = -1.0$, $P < 0.01$). As light becomes more redshifted, males display less red. Area of red coloration in males is scored from 0 (least red) to 5 (maximal red). **b**, Female detection threshold shows a significant positive correlation to λp50 ($r = 0.94$, $P < 0.05$). Females with high detection thresholds (low sensitivity) to red light mate in more redshifted habitats. Female sensitivity to red is high when the detection threshold is low and is measured in log photon flux (in units of μmol photons m^{-2} s^{-1}).
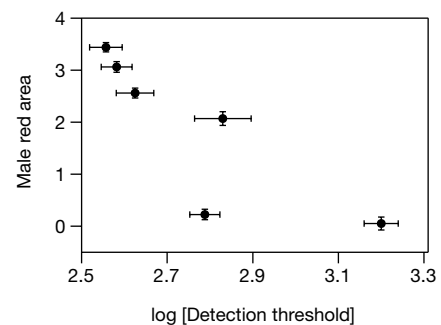

Figure 2 Relationship between female detection threshold for red and area of red coloration in males ($r = -0.94$, $P < 0.05$). Female sensitivity to red and area of red coloration in males measured as in Fig. 1.
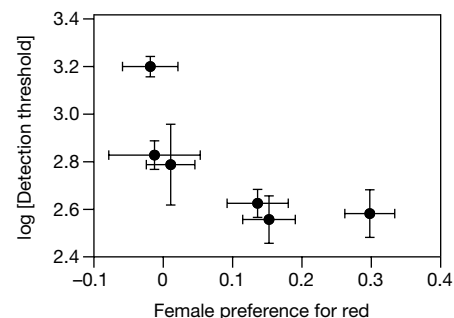

Figure 3 Relationship between female perception of red light and preference for red signals ($r = -0.94$, $P < 0.05$).

the second prediction of sensory drive.

Female sensitivity to red light correlates significantly with the area of red coloration in males (Fig. 2; $r = -0.94$, $n = 6$, $P < 0.05$), and non-significantly to red intensity ($r = -0.77$, $n = 6$, $P < 0.10$). Thus, male signals seem to be fine-tuned to female perceptual sensitivity, confirming the third prediction of sensory drive. Signal matching is also predicted by the pre-existing bias hypothesis[9]. Covariation could be caused by male signals evolving to match a pre-existing bias[9], or could arise because both traits evolved in response to a shared environment[4]; therefore, causality remains to be determined.

A critical prediction of speciation by sexual selection is that mate signals and preferences diverge and this divergence contributes to reproductive isolation. In behavioural trials, I estimated female preference functions for red nuptial colour in the six populations by measuring the number of times females examined a male's nest per min, and measured reproductive isolation as the occurrence of spawning between males and females from different populations. I used analysis of covariance (ANCOVA) to estimate preference for red males by calculating the slope of the linear regression of preference (the log of the rate of nest examinations) on area of red coloration (slope estimates: Paxton limnetic = 0.15; Enos limnetic = 0.30; Paxton benthic = 0.14; Enos benthic = 0.01; Cranby = −0.01; Brannen = −0.02; slope heterogeneity $F_{5,135} = 2.3$, $P < 0.05$). Limnetics from both lakes differ significantly from other populations ($F_{1,135} = 53.3$, $P < 0.001$) and black populations differ significantly from red ones ($F_{1,135} = 7.9$, $P < 0.01$). Thus, the strength of female preference for red signals has diverged among populations. Divergence in preference for red depends, in part, on perceptual sensitivity to red (Fig. 3; $r = -0.94$, $n = 6$, $P < 0.05$).

Next, I used logistic regression to estimate spawning rates between each pair of populations, correcting for differences between populations in male propensity to spawn. I corrected all population trait means for phylogenetic similarity[19]. I then analysed the relationship between the divergence in sexually selected traits (male signals and female preferences) and reproductive isolation using generalized least squares (GLS)[19] and Mantel tests, using the six populations as replicates.

The divergence I found in both male signal colour and female

preference for red are significantly correlated with the extent of reproductive isolation between populations (Fig. 4). The extent of divergence in male signals is negatively correlated with the amount of reproductive isolation by both GLS ($b = -0.11$, $n = 6$, $P < 0.001$) and Mantel ($r = -0.93$, $P < 0.03$) tests. I found a similar pattern for divergence in female preference and reproductive isolation with both GLS ($b = -0.87$, $n = 6$, $P < 0.05$) and Mantel ($r = -0.90$, $P < 0.05$) tests. Thus, greater divergence in male signals and female preference contributes to greater reproductive isolation between populations.

Body size is also known to contribute to reproductive isolation between ecotypes[20], but differences in body size do not account for the pattern shown in Fig. 4. Paxton benthics and limnetics differ most in body size[20] and should have the lowest spawning rate; however, they spawn at nearly twice the rate of Enos benthics and limnetics (Paxton benthics and limnetics = 0.30; Enos benthics and limnetics = 0.17). Results are consistent with sensory drive predictions, but both Fisherian runaway[1,2] and condition-dependent[21] hypotheses predict a correlation between male signal and female preference and could contribute to this correlation. Neither hypothesis makes specific predictions about female perception. However, the signalling environment strongly influences both traits, which is only indirectly predicted for male colour by the Fisher process if the strength of natural selection opposing mate choice is negatively correlated with water colour. Enhancing conspicuousness in the local environment is likely to increase predation risk, so runaway selection should produce a pattern opposite to the one observed here. Condition dependence predicts the relationship between male colour and environment if the cost–benefit relationship of signalling varies closely with water colour, or if carotenoid availability correlates negatively with water colour. A model that considers the interaction between condition dependence and perception predicts the pattern found; however, this prediction arises from effects of environment on signal detectability[22] and thus invokes a mechanism similar to sensory drive.

Perception, preferences and signals diverge in correlation with habitat, implying that some habitat specialization may precede or coincide with their divergence. Ecological diversification and repro-
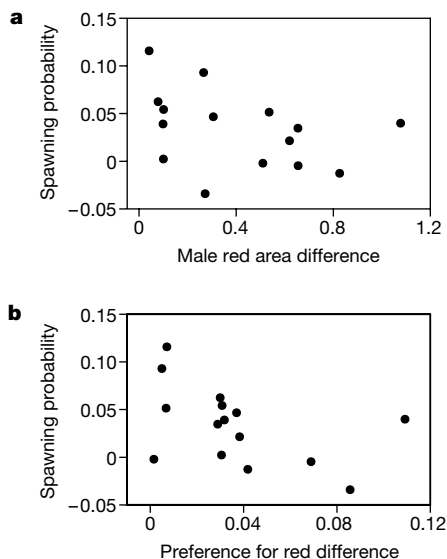

Figure 4 Relationship between the divergence among populations in male signal colour and female preference for red, and reproductive isolation between populations. Values given are for pairs of populations and are corrected for phylogeny. **a**, Difference in area of red coloration in males correlates negatively with spawning probability. **b**, Difference in strength of female preference for red signals correlates negatively with spawning probability. For both traits, as the extent of divergence increases the probability of mating decreases significantly with both GLS and Mantel analyses. See text for details.

ductive isolation are probably both necessary for the persistence of species with currently parapatric or sympatric distributions, and their joint occurrence is a feature of several models of speciation[23,24]. Assortative mating on the basis of a trait correlated with resource specialization, such as body size, also occurs in these stickleback populations[20]. The combined forces of divergent sexual selection and competition for resources in sticklebacks[25] are expected to facilitate the rapid evolution of phenotypic differences and speciation[26].

Closely related species often differ markedly in sexually selected traits. Understanding the role sexual selection has in speciation requires that we identify both the causes of diversity in sexually selected traits and the consequences on pre-mating isolation. My results support important predictions of the hypothesis that sexual selection facilitates speciation, and provide evidence that sensory drive is a critical selective mechanism. The environment is implicated: when local habitats differ, divergence in sexually selected traits is a likely result. Thus, sensory drive provides a general mechanism for divergence in signalling systems, and could figure prominently in the speciation process. □

Methods

Measuring ambient light

I measured spectral radiance in nesting habitats of the six populations with a spectro-radiometer (Licor underwater (UW1800) or Ocean Optics (S2000)). At two sites in each habitat where males were observed nesting I recorded sidewelling light (perpendicular to the water surface) at the approximate nesting depth (0.3–2 m). I calculated λp50 values from spectral radiance curves by integrating the area under the curves and taking the median value[27]. I analysed λp50 values with an analysis of variance (ANOVA) test.

Measuring male colour

Just before conducting trials I scored the area and intensity of red on each male used in mating trials according to a six-point scale from 0 (no red area; no red intensity) to 5 (maximal red area; maximal intensity). The maximal area of red coloration included colour on the male's lips, throat, gill covers, and ventral surface (extending back to the anal spines). I used single-degree-of-freedom contrasts to test for differences between populations in male colour. Sample sizes: Paxton limnetic = 34; Enos limnetic = 27; Paxton benthic = 31; Enos benthic = 26; Cranby = 22; Brannen = 23; total = 163.

Measuring female perception

I used a behavioural psychophysical technique relying on the optomotor response[18] to assay female perceptual sensitivity to red light. I used a standard slide projector fitted with a rotating spoked wheel to create a moving visual field; a narrow band 10-nm interference filter (640nm; PTR Optics) to control wavelength; and neutral density filters (PTR Optics) to control light intensity. Fish were light-adapted under a 60-W broad-spectrum bulb (Bulbrite Industries true daylight) for 20 min before testing. My response criterion was that the fish follow the rotation of stripes at the rotational speed ($6°$ s^{-1}). I used a descending method of limits procedure[28] with 0.3 log unit decrements and estimated the detection threshold as the light intensity one step above that at which the fish ceased responding to the stimulus. After the fish stopped responding I increased light intensity by one step to determine whether the fish would resume response. I then ascertained this light intensity value with a LiCor 1800 spectroradiometer to determine the absolute threshold values (log of light intensity in units of μmole photons m^{-2} s^{-1}). I used single-degree-of-freedom contrasts to test for differences between ecotypes and between populations with black or red males. Sample sizes: Paxton limnetic = 82; Enos limnetic = 92; Paxton benthic = 61; Enos benthic = 99, Cranby = 54; Brannen = 61; total = 449.

Measuring female preference

I used no-choice mating trials to assess female preferences for male colour. After a single male had built a nest in a 100-l aquarium I introduced a single gravid female to the aquarium (see refs 20, 29 for details). I scored male colour before each trial. During the 20-min trials I collected data on female response to male courtship and the occurrence of spawning. After each trial I measured female perceptual sensitivity, body size and weight, and verified that the female was ready to spawn. I included only those trials where females were receptive. I estimated female preference functions by ANCOVA with area of red coloration as the covariate and female population as a categorical effect. I calculated the linear regression coefficient of rate of nest examination on area of red coloration for each female population on the basis of trials conducted with males from the females' own population. These slope estimates indicate the strength of preference for male nuptial colour for each female population. Sample sizes: Paxton limnetic = 29; Enos limnetic = 17; Paxton benthic = 23; Enos benthic = 23; Cranby = 26; Brannen = 34; total = 152.

Reproductive isolation and divergence

I used no-choice mating trials, as above, to measure reproductive isolation, pairing males

and females from different populations (for example, Paxton limnetic × Paxton benthic; Enos benthic × Brannen). Total sample size was 654. I used logistic regression to estimate spawning rates between each pair of populations, correcting for differences between populations in male propensity to spawn. Next, I estimated the magnitude of divergence in sexually selected traits by calculating the difference between pairs of populations in male signal (red area) and strength of preference for red (slope estimates). This yields 15 pairwise comparisons. I corrected all values for phylogenetic similarity. To do this, I calculated the inverse of the sum of the branch lengths between each pair of populations from a phylogenetic tree[30], and used these values as weighting factors. I then analysed the relationship between the divergence in sexually selected traits (male signals and female preferences) and reproductive isolation using GLS[19] and Mantel tests. I used the six populations as replicates.

1. Fisher, R. A. *The Genetical Theory of Natural Selection* (Clarendon, Oxford, 1930).
2. Lande, R. Models of speciation by sexual selection on polygenic traits. *Proc. Natl Acad. Sci. USA* **78**, 3721–3725 (1981).
3. West-Eberhard, M. J. Sexual selection, social competition, and speciation. *Q. Rev. Biol.* **58**, 155–183 (1983).
4. Endler, J. A. Signals, signal conditions, and the direction of evolution. *Am. Nat.* **139**, 125–153 (1992).
5. Ryan, M. J. & Wilczynski, W. Evolution of intraspecific variation in the advertisement call of a cricket frog (*Acris crepitans*, Hylidae). *Biol. J. Linn. Soc.* **44**, 249–271 (1991).
6. Marchetti, K. Dark habitats and bright birds illustrate the role of the environment in species divergence. *Nature* **362**, 149–152 (1993).
7. Seehausen, O., van Alphen, J. J. M. & Witte, F. Cichlid fish diversity threatened by eutrophication that curbs sexual selection. *Science* **277**, 1808–1811 (1997).
8. Levine, J. S. & MacNichol, E. F. Jr Visual pigments in teleost fishes: effects of habitat, microhabitat, and behavior on visual system evolution. *Sensory Process.* **3**, 95–131 (1979).
9. Ryan, M. Sexual selection, sensory systems, and sensory exploitation. *Oxf. Surv. Evol. Biol.* **7**, 156–195 (1990).
10. McFarland, W. N. & Munz, F. W. Part III: The evolution of photopic visual pigments in fishes. *Vision Res.* **12**, 1071–1080 (1975).
11. Reimchen, T. E. Loss of nuptial color in threespine sticklebacks (*Gasterosteus aculeatus*). *Evolution* **43**, 450–460 (1989).
12. Lythgoe, J. N. *The Ecology of Vision* (Oxford Univ. Press, 1979).
13. Endler, J. A. Variation in the appearance of guppy color patterns to guppies and their predators under different visual conditions. *Vision Res.* **31**, 587–608 (1991).
14. McPhail, J. D. Ecology and evolution of sympatric sticklebacks (*Gasterosteus*): morphological and genetic evidence for a species pair in Enos Lake, British Columbia. *Can. J. Zool.* **62**, 1402–1408 (1984).
15. McPhail, J. D. Ecology and evolution of sympatric sticklebacks (*Gasterosteus*): evidence for a species pair in Paxton Lake, Texada Island, British Columbia. *Can. J. Zool.* **70**, 361–369 (1992).
16. McPhail, J. D. in *The Evolutionary Biology of the Threespine Stickleback* (eds Bell, M. A. & Foster, S. A.) 399–437 (Oxford Univ. Press, 1994).
17. Schluter, D. in *Endless Forms: Species and Speciation* (eds Howard, D. J. & Berlocher, S. H.) 114–129 (Oxford Univ. Press, 1998).
18. Cronly-Dillon, J. & Sharma, S. C. Effect of season and sex on the photopic spectral sensitivity of the three-spined stickleback *J. Exp. Biol.* **49**, 679–687 (1968).
19. Martins, E. P. & Hansen, T. F. Phylogenies and the comparative method: a general approach to incorporating phylogenetic information into the analysis of interspecific data. *Am. Nat.* **149**, 646–667 (1997).
20. Nagel, L. & Schluter, D. Body size, natural selection, and speciation in sticklebacks. *Evolution* **52**, 209–218 (1998).
21. Kodric-Brown, A. & Brown, J. H. Truth in advertising: the kinds of traits favored by sexual selection. *Am. Nat.* **124**, 309–323 (1984).
22. Schluter, D. & Price, T. D. Honesty, perception, and population divergence in sexually selected traits. *Proc. R. Soc. Lond. B* **253**, 117–122 (1993).
23. Lande, R. & Kirkpatrick, M. Ecological speciation by sexual selection. *J. Theor. Biol.* **133**, 85–98 (1988).
24. Higashi, M., Takimoto, G. & Yamamura, N. Sympatric speciation by sexual selection. *Nature* **402**, 523–526 (1999).
25. Schluter, D. Experimental evidence that competition promotes divergence in adaptive radiation. *Science* **266**, 798–801 (1994).
26. Podos, J. Correlated evolution of morphology and vocal signal structure in Darwin's finches. *Nature* **409**, 185–188 (2001).
27. McDonald, C. G. & Hawryshyn, C. W. Intraspecific variation of spectral sensitivity in threespine stickleback (*Gasterosteus aculeatus*) from different photic regimes. *J. Comp. Physiol. A* **176**, 255–260 (1995).
28. Klump, G. M., Dooling, R. J., Fay, R. R. & Stebbins, W. C. *Methods in Comparative Psychoacoustics* (Birkhauser, Basel, Switzerland, 1995).
29. Rundle, H. D., Nagel, L. M., Boughman, J. W. & Schluter, D. Natural selection and parallel speciation in sympatric sticklebacks. *Science* **287**, 306–308 (2000).
30. Taylor, E. B. & McPhail, J. D. Historical contingency and ecological determinism interact to prime speciation in sticklebacks, *Gasterosteus. Proc. R. Soc. Lond. B* **267**, 2375–2384 (2000).

Acknowledgements

Correspondence and requests for materials should be addressed to J.W.B. (e-mail: boughman@zoology.ubc.ca).

....

Nodulation of legumes by members of the β-subclass of Proteobacteria

Lionel Moulin, Antonio Munive, Bernard Dreyfus & Catherine Boivin-Masson

Laboratoire des Symbioses Tropicales et Méditerranéennes, IRD-INRA-CIRAD-ENSAM Baillarguet, PB 5035, 34398 Montpellier Cedex 5, France

....

Members of the Leguminosae form the largest plant family on Earth, with around 18,000 species. The success of legumes can largely be attributed to their ability to form a nitrogen-fixing symbiosis with specific bacteria known as rhizobia, manifested by the development of nodules on the plant roots in which the bacteria fix atmospheric nitrogen, a major contributor to the global nitrogen cycle. Rhizobia described so far belong exclusively to the α-subclass of Proteobacteria, where they are distributed in four distinct phylogenetic branches[1,2]. Although nitrogen-fixing bacteria exist in other proteobacterial subclasses, for example *Herbaspirillum* and *Azoarcus* from the phylogenetically distant β-subclass, none has been found to harbour the *nod* genes essential for establishing rhizobial symbiosis[3,4]. Here we report the identification of proteobacteria from the β-subclass that nodulate legumes. This finding shows that the ability to establish a symbiosis with legumes is more widespread in bacteria than anticipated to date.

Recent taxonomic classifications portray rhizobia as belonging to three different branches of the α-subclass of Proteobacteria: the *Mesorhizobium-Sinorhizobium-Rhizobium* branch, the *Bradyrhizobium* branch and the *Azorhizobium* branch[1,5]. We recently described a fourth rhizobial branch within the α-subclass of Proteobacteria, containing methylotrophic rhizobial *Methylobacterium*[2]. To explore further the phylogenetic diversity of nitrogen-fixing legume symbionts, we characterized a collection of rhizobia isolated from tropical legumes. We found here that two bacteria isolated from nodules of *Aspalathus* and *Machaerium* plants were very distant from known rhizobia.

Strain STM678 was originally isolated from the South African legume *Aspalathus carnosa*, which was thought to be nodulated by bacteria of the *Bradyrhizobium* genus[6]. However, we performed phylogenetic analysis of gene sequences of the small subunit of ribosomal RNA (16S rRNA), and found that strain STM678 does not belong to any of the four branches of rhizobia described so far, nor even to the α-subclass of Proteobacteria, but instead belongs to the β-subclass of Proteobacteria (Fig. 1). From this analysis, we found the most closely-related sequences to that of strain STM678 (AJ302311) to be those of *Burkholderia kururiensis* (96.9% identity), *B. brasilense* (96.8% identity) and *B. graminis* (96.8% identity). Phylogenetic analyses of partial sequences of the 23S rRNA gene (AJ302313) and the *dnaK* gene encoding the chaperon heat shock protein (AJ302314) were consistent with the 16S rRNA analysis, thus unambiguously positioning strain STM678 in the *Burkholderia* genus within the β-subdivision of Proteobacteria.

To ensure that the *Burkholderia* strain STM678 was indeed a rhizobium, we checked its ability to re-nodulate a leguminous plant. Because seeds of the original host plant, *A. carnosa*, were not available, we selected as test plant *Macroptilium atropurpureum*, a tropical legume capable of establishing a symbiosis with diverse rhizobia. Over a three-week period, strain STM678 formed 5 to 20 nodules per plant on the roots of *M. atropurpureum* (Fig. 2). The nodules displayed the classical determinate nodule structure, with a central 'infected' tissue containing cells with intracellular bacteria and a peripheral tissue with vascular bundles (Fig. 2). Single colonies re-isolated from surface-sterilized nodules exhibited the characteristics of strain STM678, as assessed by 16S rDNA sequencing and *nodA* analysis using polymerase chain reaction-restriction fragment length polymorphism (PCR-RFLP; see below). Hence, Koch's postulates were verified. To eliminate the possibility that strain STM678 is a mixture of two different bacteria, a *Burkholderia* and a rhizobium, we isolated spontaneous mutants resistant to chloramphenicol, rifampicin and streptomycin, and showed by 16S rDNA and *nodA* PCR-RFLP analyses that the individual mutants retained the characteristics of both *Burkholderia* and rhizobia. Nodules induced on *M. atropurpureum* by strain STM678 were ineffective in terms of nitrogen fixation, probably because *M. atropurpureum* is not the original symbiotic partner of strain STM678. Supporting this conjecture, strain STM678 was indeed found to contain the *nifH* gene encoding dinitrogenase reductase, a key enzyme in nitrogen fixation (AJ302315). The highest identity values with other *nifH* genes were 81.2% (the α-Proteobacterium *Azorhizobium caulinodans*) and 81.1% (the β-Proteobacterium *Herbaspirillum seropedicae*).
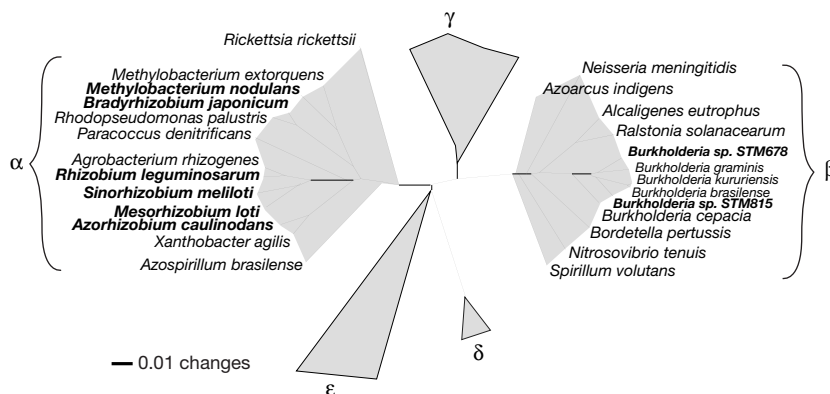

Figure 1 Unrooted 16S rDNA tree of Proteobacteria (purple bacteria). The figure shows the phylogenetic relationships between the different rhizobial genera—as represented by type species in bold—including the new rhizobial *Burkholderia* sp. strains. α, β, δ, γ and ε represent the different subdivisions of the Proteobacteria. The tree was constructed by using the neighbour-joining method and adapted from ref. 5. 16S rDNA sequences of published bacteria are available in GenBank. 16S rDNA from *Burkholderia* sp. STM 678 and *Burkholderia* sp. STM 815 are given in the text (AJ 302311 and AJ 302312).